NASA Contractor Report 168331

# EMISSION FTIR ANALYSES OF THIN MICROSCOPIC PATCHES OF JET FUEL RESIDUES DEPOSITED ON HEATED METAL SURFACES



James L. Lauer and Peter Vogel

Rensselaer Polytechnic Institute

Troy, New York


January 1984

Prepared for

NATIONAL AERONAUTICS AND SPACE ADMINISTRATION

Lewis Research Center

Under Grant NAG3-205

TABLE OF CONTENTS


FOREWORD ..... iii

1.0 SUMMARY ..... 1

2.0 INTRODUCTION ..... 1

3.0 EXPERIMENTAL ..... 3

3.1 Apparatus and Experimental Conditions of Deposit Collection ..... 3
3.2 Test Fuels ..... 4
3.3 Spectroscopic Analyses ..... 4
3.4 Calibration ..... 5

4.0 RESULTS AND DISCUSSION ..... 6

4.1 Bomb Experiments ..... 6

4.1.1 Infrared Emission ..... 6
4.1.2 Surface Enhanced Raman (SERS) Spectrum ..... 7

4.2 Lewis Thermal Stability Rig(MJFSR) ..... 8

4.2.1 Overview ..... 8
4.2.2 Dodecane Spectra ..... 8
4.2.3 Jet A and ERBS Spectra ..... 9
4.2.4 Effect of Deposition Temperature on the Spectrum of an ERBS Deposit ..... 9

5.0 CONCLUSION ..... 10

REFERENCES ..... 11

FOREWORD

This work was funded by NASA-Lewis Grant NAG 3-205. Some support was also given by ARO Grant No. DAAG 2483K0058 and by AFOSR Grant No. AFOSR-81-0005. We are very thankful to our sponsors.

The "flow-fuel" deposits were provided us by Dr. Gary Seng of NASA-Lewis, who directed the simulator work. This work and his comments and encouragements throughout this project are most gratefully acknowledged.

The assistance of Professor T.E. Furtak and his students in obtaining the Raman spectra is acknowledged.

## 1.0 SUMMARY

The objective of the investigation was to relate fuel stability with fuel composition and to develop mechanisms for deposit formation, which can account for the large influence of small concentrations of nonhydrocarbons. Fuel deposits reduce heat transfer efficiency and increase resistance to fuel flow and are therefore highly detrimental to aircraft performance. Infrared emission Fourier transform spectroscopy was chosen as the primary method of analysis because it was sensitive enough to be used in situ on tiny patches (0.1 mm diameter and less) of monolayers or of only a few molecular layers of deposits which generally proved completely insoluble in any nondestructive solvents.

The bulk of the deposits were produced by NASA on metal strips (shims) in a high pressure/high temperature fuel system simulator operated with aerated fuel at varying flow rates. The shims were mounted on a slightly heated holder in such a way that the deposits faced an all-reflecting microscope objective of high numerical aperture and long working distance, which was coupled to an FTIR spectrophotometer. Some deposits were also generated in a closed small corrosion bomb on different metal strips by heating a small amount of dodecane or toluene in air.

Deposits of four base fuels were compared; dodecane, a dodecane/tetralin blend, commercial Jet A fuel, and a broadened-properties jet fuel particularly rich in polynuclear aromatics. Every fuel in turn was provided with and without small additions of such additives as thiophene, furan, pyrrole and copper and iron naphthenates.

While the deposit weights were highest for the aromatic fuel compositions, the band intensities of C-C and C-H bands were highest for dodecane. In all cases furan and pyrrole increased weights and band intensities very strongly. Significantly, the naphthenates and tetralin, increased the intensity of the "amorphous" component of the 725/730 $cm^{-1}$ methylene rocking mode of solid paraffinic structures.

Arguments are presented for a mechanism by which the additives are concentrated on the solid surfaces and interact with oxygenated hydrocarbon radicals to form amorphous polymers.

A very thin deposit formed on silver from dodecane in the corrosion bomb was also analyzed by surface-enhanced Raman spectroscopy (SERS). Its very sharp bands were of much help in determining deposit composition. Deposit spectra and therefore compositions generated in the corrosion bomb varied considerably for aluminum, silver, and stainless steel substrates.

## 2.0 INTRODUCTION

Aircraft fuels containing oxygen often have a tendency to form hard, sticky, carbonaceous and generally insoluble deposits on contacting surfaces at elevated temperatures. Small concentrations of nonhydrocarbons, such as nitrogen- and sulfur-containing materials, often enhance the deposit-forming tendency. In aircraft gas turbine engines these deposits may clog critical

passages in valves and nozzles and decrease heat transfer efficiency through heat exchanger surfaces. These problems may increase in newer engines due to the higher temperatures and longer residence times expected with higher compression ratios and staged fuel injection. Future fuels are likely to be richer in aromatics and nonhydrocarbons than present ones and therefore likely to aggravate the deposit problems even more.

Clearly there is a need for the testing of fuels for their deposit-forming tendencies. In the longer run, however, an understanding of the mechanisms leading to deposit formation must be developed so that future fuels and engines can be designed to minimize deposit problems. Most of the testing is done today with small flow systems allowing for fuel and surface heating and the injection of controlled amounts of air or oxygen into the flowing test fuel. These JFTOT systems (Jet Fuel Thermal Oxidation Testers) typically use stainless steel or aluminum tubes, about 15 cm long, and of 0.3 cm diameter on their fuel-immersed portion for deposit collection on their outer surface. These tubes are located in the stream of test fuel and are heated by the passage of electric current. A thermocouple in the center of their hollow interior records an average temperature, but this method of heating practically insures a temperature gradient along the tube axis. Furthermore, the large curvature of the mantle surface on which fuel deposits are formed, is very inconvenient for most methods of nondestructive chemical analysis. A superior device for deposit collection was therefore constructed at NASA-Lewis, where the surfaces are flat and removable strips of metal (shims) and of relatively large size (about 2 $cm^2$), yet small enough compared to the overall flow systems to insure uniform surface temperature.

For the study reported here both these shim deposits and deposits formed in our own laboratory on similar shims in a small corrosion test bomb under stationary conditions, were used. The fuels for this study were selected to be typical of actual ones. They were used either neat or containing small concentrations of simple molecules representative of typical nonhydrocarbon contaminants. Not unexpectedly the deposits formed under stationary conditions were different from those formed under flow because of the difference in precursor or intermediate species availability. However, the former deposits were found to be different also when shims of different metals were simultaneously used and thus provided a simple--and inexpensive--procedure for evaluating substrates. Deposit formation from liquid fuels depends very strongly on the nature of the solid boundary surfaces.

In view of the complexity of the process and the very small quantities of deposits formed in reasonable test times, say a few hours, it is not surprising that the standard deposit evaluating procedure today is still visual comparison of the deposit color with those on a standard color chart. A JFTOT "Tube Deposit Rater" (TDR) by which the reflected color is compared, has also been used. Unfortunately the "color number" so found does not provide much information of a chemical nature and therefore tells us little or nothing about the nature or mechanism of deposit formation. The procedure used in this study was infrared emission Fourier microspectrophotometry (FIEMS), which is extremely sensitive and very powerful for the solution of problems in molecular and crystalline structure. Preliminary studies of aircraft fuel deposits by FIEMS were reported previously [1] so that the apparatus and its capabilities need only a brief description. The results of the flow experiments showed that both the quantity and the nature of the deposits

are altered with change of fuel composition and to some extent, change of nonhydrocarbon additive ("spike"). A strong influence of the substrate was shown in the bomb experiments.

In one instance, surface-enhanced Raman spectroscopy (SERS) was used to analyze a bomb deposit formed from dodecane on a silver surface. Because it is the first application of SERS to a "real" material, the very respectable spectrum is communicated here also.

## 3.0 EXPERIMENTAL

### 3.1 Apparatus and Experimental Conditions of Deposit Collection

Figure 1 is a photograph of the Modified JFTOT Flat Sample Rig (MJFSR) [1]. For this work it is important to note that the test specimens (shims) had a rectangular area of 10 x 20 mm exposed to the flowing fuel. Since the deposit weights varied between 0.02 and 0.2 mg (Figure 9) and their density was estimated as close to unity (between polyolefins and phenolic resins), thicknesses of 1000 Å to 1 μm could be estimated. These values are similar to our previously estimated values of 1000 Å, which were arrived at by scanning electron microscopy (SEM, [2]). Since these weights were obtained by differential weighings and represent small differences between relatively large numbers, their accuracy is not high. The higher weights were usually observed when naphthenates had been added to fuels. These materials are surfactants and caused deposits to be formed on both sides of the shims.

The conditions of the MJFSR runs were: test duration 120 minutes and run temperature 250°C. Since the heat-up and cooling times were excluded from the formal test duration and the temperatures were recorded at different locations on the outlet side, the actual test conditions were deduced by interpolations or small extrapolations. In any case the same conditions were always achieved and maintained to better than one percent (± 1%).

Work is now in progress to determine deposit thicknesses by ellipsometry.

For the stationary experiments in our laboratory a standard 500 mℓ stainless steel corrosion bomb was used. It was provided with inert (silicone or Viton) gaskets and filled with 10 mℓ of hydrocarbon test fluid; then several shims were inserted, and the bomb was heated to and maintained at 250°C for three hours. The hydrocarbon was in large excess over the oxygen and complete combustion was excluded, in analogy to the situation of the MJFSR where aerated fuels are used. The conditions of the bomb experiments insured that the metal strips (shims) suspended within the bomb were at uniform temperature throughout and at the same temperature as the fuel. Differences in amount and character of the material deposited on these strips must therefore be attributed exlusively to differences in the strip material deposited on these strips must therefore be attributed exclusively to differences in the strip material and cannot be attributed to temperature gradients, for example.

The deposit samples obtained from the MJFSR were all collected on commercial stainless steel foil and the same foil was also employed in the bomb experiments. However, in the latter strips of aluminum foil and silver foil

were also used as deposit collectors. For the Raman experiment a microscope slide covered with a thin evaporated silver film ("island film") was momentarily dipped into the test fluid after the test. The bomb deposit samples were very much thinner than the MJFSR ones, for they were barely visible as a change of reflectivity. The roughness of the stainless steel foil was far greater (at least three times) than that of the aluminum and silver foils; the roughness of the aluminum foil was about 50% greater than that of the silver foil. These estimates are based on the graybody background intensities in infrared emission.

## 3.2 Test Fuels

Three base fuels were used in the MJFSR: 1) Jet A, a representative jet fuel consisting of about 17% by volume of mononuclear aromatics, 0.1% of olefins, 2% of naphthalenes, and the balance of saturates; 2) ERBS, an experimental broadened-properties reference fuel, consisting of 13% mononuclear aromatics, 12% dinuclear aromatics, 2% polynuclear aromatics, 0.3% olefins and the balance of saturates; and 3) dodecane, an essentially pure hydrocarbon (aromatic and olefinic impurities less than 0.03%). In addition, a few runs were made with a mixture of 80% dodecane and 20% tetralin. Tetralin is well known for its peroxide-forming tendencies and a preliminary study of its influence on the formation and composition of the deposits was thought to be worth including.

The "spikes" or additives were tested in the MJFSR in varying concentrations. They were thiophene, furan, pyrrole and copper and iron naphthenates. For Jet A and ERBS the concentrations were: pyrrole 0.1 wt%, thiophene and furan 1.0 wt%, copper naphthenate 2PPM and iron naphthenate 1 PPM. For dodecane all the amounts were twice the above. Thiophene and pyrrole were thought to be good initial representatives of nonhydrocarbon components in fuel. The naphthenates were used because it was thought that a portion of the metals present in fuels are in organometallic form. However, the naphthenates can behave like soaps and alter the flow pattern at boundary surfaces.

Only two hydrocarbon liquids were used in the bomb experiments, dodecane and toluene.

## 3.3 Spectroscopic Analyses

Our preferred method of analysis was essentially the same Fourier emission microspectrophotometry we had used previously [2]. The schematic drawing of Figure 2 was taken from our previous publication. However, a number of improvements were made. Thus, for example, the chopper and the blackbody were relocated to a position between the heated sample and the lens. The old position below the lens, chosen for reasons of space and convenience, would lead to increased background radiation as the lens would heat up and itself become a source of radiation. This problem became particularly acute when the sample temperature was raised from 40°C to 130°C to improve the signal/noise ratio of extremely thin deposits. The tuning fork chopper was replaced by a rotating wheel at 45 degrees with the optical axis of the lens to introduce sample and blackbody radiation alternatingly into the spectrometer. The wheel was more stable and a better reflector than the tuning fork tines. However, perhaps the most important innovation of primary importance for

the analysis of the extremely thin deposits produced in our bomb experiments was a heated sample holder that would allow the planes of the shims to be placed at a high angle with the optic axis. Doing that also required a lens of longer working distance than the one used previously. A large angle of emission is of great importance when very thin samples on metal surfaces are analyzed by infrared emission, for then the metal surfaces produce an intensity pattern that has its maximum at viewing angles of 70°-80° from the surface normal (Greenler [3]).

Introduction of a variable viewing angle thus added another element of complexity in our sample location system. It is not important to describe it in detail in this paper, but it should be mentioned that a region in a deposit sample can be reproducibly located by X,Y,Z and rotational adjustments in both a horizontal and a vertical plane to about ±0.05 mm and 0.1° of angle. To make use of this precision all the instrumentation is set on an optical table of high quality. Depending on the objective lens used the deposit area viewed can be varied from about 1 $cm^2$ to 100 $\mu^2$, so that small spots of deposit can be analyzed.

In the work reported here polarization modulation was not used. The viewing angle was kept between 45 and 75°, with respect to the surface normal. The influence of viewing angle on a typical deposit spectrum is shown in Figure 3. At 0° very little structural detail appears above the background. At 45° strong bands at 1470, 1610, 1730 and 1780 $cm^{-1}$ are very distinct. These bands can be assigned to be $CH_2$ scissoring mode, the asymmetrical stretch of carboxylic acid salts, and the C=O stretches of ketones and p-lactones, respectively. As pointed out by Greenler [2], the most intense emission bands from a material adsorbed in a thin layer on a metal surface are likely to be those originating from a transition dipole vector having a strong component vibrating perpendicularly to the surface.

Our slow-scanning Fourier spectrometer is ideally suited for the analysis of the very weak infrared emissions (small sample areas, sample temperature as low as 40°C with a room temperature detector and very thin samples on metal surfaces) [4], but practical considerations allow the averaging of only a few (three or four) spectra. In general, only the spectral region from 600 to 2000 $cm^1$ could be used because of the rapid radiation intensity fall-off at higher frequencies. Furthermore, it proved to be convenient to separate this spectral region into three parts of optical filtering (600-1200, 1100-1400, and 1300-2000 $cm^{-1}$) to reduce the dynamic range. Not all ranges were run for all the spectra. The reciprocal resolution was ±5 $cm^{-1}$. The last two ranges required complete removal of moisture and carbon dioxide from the spectrometer atmosphere.

The Raman spectra were obtained with a Spex spectrometer in the RPI Physics Department.

### 3.4 Calibration

Figure 4 shows an emission spectrum of a 2.5 μm thick film of Mylar at 60°C. It is included here not only to show that all the absorption bands are clearly distinguishable as emission bands and that they appear at the same frequencies but also the three spectral ranges we use, which are separated by optical filters of sharp cutoffs. That the spectrum was not ratioed to

the blackbody, is one reason that the relative intensitites of the various bands are not those observed in absorption. Another reason for the intensity differences is the effect of the substrate and polarization.

The Mylar spectra are single spectra, not averages of many spectra as has become common practice in Fourier infrared spectroscopy.

## 4.0 RESULTS AND DISCUSSION

### 4.1 Bomb Experiements

#### 4.1.1 Infrared Emission

Figures 5 and 6 contain three infrared emissions each of deposits from dodecane and toluene, which were collected simultaneously on stainless steel, aluminum and silver strips. Thickness data are lacking, but visual comparison with deposits on tubes, whose thickness was estimated by scanning electron microscopy, would seem to indicate that these strip deposits were less than 100 Å thick. The spectra of these figures were all normalized and displaced vertically in the order of background intensity, stainless steel furnishing the highest background, no doubt because it is the poorest reflector and had the roughest surface. It should also be pointed out that all these spectra were separately obtained in three separate wavenumber regions although the composite spectra of Figures 5 and 6 appear to be continuous. Casual comparison of the spectra shows that the contrast is highest for the aluminum deposits and lowest for the stainless steel deposits, the silver deposit spectra occupying an intermediate position. The order of the spectral contrasts parallels that of the reflectivity of the substrate in the infrared (in the infrared aluminum is a somewhat better reflector than silver).

The strongest and most outstanding emission band in the spectra of the aluminum deposits formed from both dodecane and toluene is peaking at 930 $cm^{-1}$ for the former and at 910 $cm^{-1}$ for the latter. A weaker band in this spectral range is also present in all the other spectra. For this reason and because of the wavenumber difference it is unlikely that this band is merely the alumminum oxide phonon described by Mertens [5]. The chances are that it is both due to this phonon and to the OH...O out-of-plane hydrogen deformation of the carboxyl dimer. This assignment is confirmed by a strong band at 1300-1310 $cm^{-1}$, which is present in all the dodecane deposit spectra but only in the toluene deposit spectrum for aluminum. This band is considered to be caused by the C-O stretch of the carboxyl. Another carboxyl dimer band, the C=O stretch expected to be located between 1680 and 1740 $cm^{-1}$ is strongly present in both of the aluminum deposit spectra. The aluminum deposit spectra also contain a strong band at 1580 $cm^{-1}$ and a weaker one at 1430 $cm^{-1}$, which are usually assigned to the asymmetric and symmetric stretching modes of carboxylic acid salts, as well as a strong band at 1650 $cm^{-1}$, which can be assigned to C=C (olefin) stretch. The presence of a carboxylic acid in the aluminum deposits from dodecane is also indirectly confirmed by the series of nearly equispaced bands between 1200 nd 1320 $cm^{-1}$, which represent the harmonics of the $CH_2$ wagging mode; these bands are usually particularly intense in paraffinic carboxylic acids and salts. On the other had, the toluene deposits on aluminum show characteristic bands near 1580 and 1630 $cm^{-1}$, at 710 $cm^{-1}$ and around 1450 and 1500 $cm^{-1}$, which can be assigned to

the phenyl group. A band near 710 $cm^{-1}$ in all the dodecane deposits is likely to be the $CH_2$ rock. A band near 1730 $cm^{-1}$ for the dodecane deposits and near 1700 $cm^{-1}$ for the toluene deposits must be assigned to carbonyl.

There is much less evidence for carboxylic acids and little if any, for salts in the silver deposits and essentially none for either in the stainless steel deposits. In the latter the most identifiable bands, i.e., 1260 and 1350 $cm^{-1}$ for dodecane are $CH_2$ and $CH_3$ deformations. The silver deposit spectra, however, do show carbonyl bands as well.

The spectra of the bomb deposits can therefore be summarized as follows: On aluminum the hydrocarbons were partly oxidized all the way to carboxylic acids and salts, and partly to aldehydes and ketones, on silver also partly to carboxylic acids and to aldehydes and ketones and on stainless steel probably mostly to hydrocarbon polymers. The latter spectra show little evidence of the presence of carbonyl groups.

How do these spectra compare with the MJFSR spectra? A good example is shown in Figure 7.

Dodecane deposits on stainless steel are compared for the two situations. If at all present the 1260 and 1350 $cm^{-1}$ bands of the bomb experiments are essentially absent for MJFSR. However the MJFSR spectrum does show possible evidence for C=O bands at 1700, 1730 $cm^{-1}$ and a strong band at 840 $cm^{-1}$ may be indicative of olefin epoxidation. Olefins are also very likely present, as evidenced by bands near 1600 $cm^{-1}$. It would appear therefore that oxidation went further in MJFSR than in our bomb.

Unfortunately our emission spectra regions do not extend beyond 2000 $cm^{-1}$ because the available energy is too low beyond that frequency. Others encountered the same limitation (Suetaka [6]).

### 4.1.2 Surface Enhanced Raman (SERS) Spectrum

The Raman spectrum of Figure 8, obtained by momentarily dipping a silver-coated microscope slide into the partly oxidized dodecane after the bomb test, was surprising for its quality. The deposit was barely visible as a minute reflectivity change and was probably no more than a few molecular layers thick. It shows strong bands at 820, 960, 1130, 1250, 1380, 1560, 1600 and at 1640 (strong) $cm^{-1}$. The principal infrared emission bands in the dodecane deposit on silver (Figure 5) are at 850, 910, 980, 1130, 1180, 1260, 1600, 1650 (weak) and 1730 $cm^{-1}$. Perhaps the most outstanding difference between these spectra is the clear absence of a Raman band at 1700 $cm^{-1}$ and the presence of broad and strong Raman bands but weak infrared bands grouped near 1400 and 1640 $cm^{-1}$. Since the carboxylic acid dimer is centrosymmetric, the asymmetric carbonyl stretch would be expected to fall at 1700 $cm^{-1}$ and be infrared-active only and the symmetric stretch to fall at 1640 $cm^{-1}$ and be Raman-active only. An infrared band near 1600 $cm^{-1}$ and a Raman band near 1400 $cm^{-1}$ are similarly expected for the coupled oscillators in carboxylic acid salts. Other bands in both the infrared and Raman spectra can be assigned to olefins and alkanes as shown in Table 1, which summarizes the data.

There is a great deal of recent literature on different selection rules for SERS and for ordinary Raman spectroscopy [7]. Some authors consider chemisorption a prerequisite for SERS. Our data would still be consistent with the assignments made, but no conclusions should be made on the basis of relative band intensities.

## 4.2 Lewis Thermal Stability Rig (MJFSR) Spectra

### 4.2.1 Overview

Figure 9 is a comparison of the deposit weight on the standard 2 $cm^2$ stainless steel surface and the "greatest unnormalized amplitude" (GUA) of our infrared emission spectra in the 650 - 1250 $cm^{-1}$ wavenumber region. This region includes essentially only bands representing C-C or C-H vibrational modes and the overall intensity in this region would be expected to be related only to carbonaceous, i.e., not oxidized, material. Some of the bars for the deposit weights are only partly filled to indicate that the measurements are possibly invalid; material crept under the sample shim. It is clear that the spikes (i.e., the additives) increased deposit weights considerably, especially thiophene, furan, and pyrrole, but the naphthenates had only little influence, presumably because of their lower concentrations, if the questioned data are excluded. The GUA's parallel the deposit weights in a general way, e.g., the GUA for the blanks (i.e., deposits from the neat fuel) are relatively low, but they are not proportional to them. The ratio of GUA to weight is high for the blanks and the deposits from the naphthenate spikes, but is much lower for the other spikes. If the lengths of the bars for the GUA's are added for a given fuel, then dodecane comes out first, ERBS fuel second and JETA third, but if the same is done for the deposit weights, ERBS fuel is first and JETA and dodecane about the same. What these comparisons show is the different nature of the deposits, thick deposits do not necessarily give intense spectral bands. The aromatic fuels contain less hydrogen per unit mass than the paraffinic and also give rise to aromatic deposits whose infrared emission bands are therefore weaker in the C-H region. Visual inspection of the deposit layers on the shims shows the difference in their nature by slightly different colors.

### 4.2.2 Dodecane Spectra

Figure 10 shows 600 - 2000 $cm^{-1}$ emission spectra of dodecane deposits formed at MJFSR on stainless steel shims. These spectra are included to show the complexity and the effect of the additives. Perhaps the single most important difference to be noticed in these spectra is the enhancement of a band at 1580 $cm^{-1}$ relative to its neighbors by the additives furan and the naphthenates. With the copper naphthenate spike this band is already the strongest in the spectrum, but with iron naphthenate this band is the outstanding feature in the 1400 - 2000 $cm^{-1}$ spectral region.

As mentioned earlier, the 1580 $cm^{-1}$ band was assigned to carboxyl salts. Therefore, the naphthenates, in particular, would seem to concentrate in the deposits.

To show the effect of the spikes more clearly the difference spectra of Figure 11 were plotted by computer. These spectra take into account that different spectra have different overall intensities. In all cases the deposit

spectrum derived from pure dodecane was substracted from the spectra derived from dodecane containing the spikes. Contributions of the spikes are pointing up, subtractions down. It will be noticed that all the additives enhance bands near 770 $cm^{-1}$, 1400, 1450 and 1550 $cm^{-1}$. Iron naphthenate and furan resolve the 1550 $cm^{-1}$ band from its 1580 $cm^{-1}$ neighbor. These bands occur in the additives. Thus the spectra show an increased concentration of additive material in the deposits.

The first two small emission bands on the left right after the steep initial rise of the background (caused by the optical filter) should also be compared in the spectra of Figure 10. These bands, located at 720 and 730 $cm^{-1}$ represent the "amorphous" and "crystalline" components of the $CH_2$ rocking mode of paraffinic chains. In the liquid phase only the 720 $cm^{-1}$ component is present. The "crystalline" mode arises from interactions between neighboring chains. Clearly the naphthenates enhanced the 720 $cm^{-1}$ band but virtually wiped out the other component. Tetralin did the same. These bands may therefore be related to the relative stickiness of the deposits.

### 4.2.3 Jet A and ERBS Spectra

In Figures 12 and 13 600 - 2000 $cm^{-1}$ emission spectra and their differences for Jet A are shown. When the "blank" is compared with the deposits from the spiked fuels, it will be noticed that the 720, 780, 850 $cm^{-1}$ triplet corresponding to aromatic substitution is reduced in relative importance by the naphthenates (it should be remembered that these are normalized spectra) while the 1580 $cm^{-1}$ carboxyl salt band is relatively enhanced. Again the conclusion is that these spikes concentrate on the surface.

The conclusions drawn from the ERBS emission spectra of Figures 14 and 15 are similar. The spikes enhance the 1580 $cm^{-1}$ carboxyl salt band, showing their increased concentration there.

### 4.2.4 Effect of Deposition Temperature on the Spectrum of an ERBS Deposit

Figure 16 shows an ERBS deposit spectrum obtained at 500°F and one at 600°F in the MJFSR. The strong aromatic bands at 1600 (naphthalene) and 1150 (m-substitution) $cm^{-1}$ are similar in both spectra. However, the higher temperature deposit also show strong bands at 720 and 780 $cm^{-1}$ which, if they belong to the same species, are characteristic of vicinal trisubstituted benzenes (fused polyphenyls?). An enhancement of these materials would be expected in the deposit, but confirmation of this result will be required.

## 5. CONCLUSION

If the reader has got the impression of enormous complexity, he has got the correct impression. Even a relatively simple, pure hydrocarbon such as dodecane can give rise to various polymeric and oxidized reaction products in its deposits and the distribution of these products depends on the nature of the collecting surface as well. The basic mechanism of liquid phase oxidation, viz. formation of alkyl hydroperoxides by the reaction of alkylperoxy radicals with hydrogen atom donors, which can be the hydrocarbon itself, has been well established [8]. In some instances peroxides are formed instead

of hydroperoxides. The decomposition of these peroxides then leads to unsaturates, aldehydes, ketones and acids with the strong possibility of chain reaction stimulations leading to polymers. The metal substrate can influence the deposit reaction, such as salt formation with carboxylic acid group. Our bomb experiments showed that an aluminum surface favors carboxylic acid formation, in other words more oxidation, and oxidative properties of aluminum oxide have been reported [9]. Since all the substrates in the bomb experiments were at constant temperature, their influence on deposit composition could be distinguished.

The MJFSR deposits were more highly oxidized, e.g., had more carboxyl groups, than the stationary bomb deposits, presumably because (i) more oxygen was available (it was continuously injected into the stream) and (ii) oxidized intermediates could be carried by convection as well as by diffusion. Hence the different compositons can be easily accounted for.

The Raman spectra (SERS) came out surprisingly well and were very helpful in the interpretation of infrared deposit spectral data. However, the procedure is clearly not routine and seems to work only with silver substrates, which are not realistic.

Much more realistic is the effect of the additives or spikes. Furan, thiophene and pyrrole are all very "aromatic" in their chemical behavior. They all promote deposit formation; pyrroles, e.g., were found to react strongly with peroxides to form polymeric sediments [10], but the detailed mechanism is unknown. Tetralin also reacts with peroxy radicals, even with its own hydroperoxy radical by serving as a hydrogen atom door, to form hydroperoxides [11]. The soluble copper and iron naphthenates are oxidation catalysts as well as micelle-formers like soaps. Dissolved copper in lubricating oils was found to be a good chain-initiation catalysts, dissolved iron a good chain-branching catalyst. Micelle formation of dissolved copper has been considered the reason for the maximum oxidation rate observed with increased concentration. Thus the naphthenates would also promote carboxylic acid formation from fuel and these acids would chemisorb on metal surfaces.

As was shown by one example, temperature can have a profound influence on surface deposits; higher temperatures increase the oxidation rate.

Thus fuel composition, temperature, the nature of the boundary surfaces and small amounts of nonhydrocarbons can be of great importance with regard to fuel stability and wall deposits. Oxidation is the prime chemical cause. And the spectroscopic procedures of infrared emission and Raman (SERS) spectroscopy can assist in differentiating between good and bad actors and in establishing mechanims.

## REFERENCES


1. Cohen, S.M., "Fuels Research-Thermal Stability Overview," NASA Conference Publication 2146, pp. 161-168 (April 1980).

2. Lauer, J.L. and Keller, L.E., "Oxidized Aircraft Fuel Deposits on Metal Surfaces Studied by Polarization-Modulated Fourier Infrared Emission Microspectrophotometry," Applications of Surface Sciences, 15, 50-65 (1983).

3. Greenler, R.G., "Light Emitted from Molecules Adsorbed on a Metal Surface," Surface Science, 69, 647-652 (1977).

4. Griffith, P.R., Chemical Infrared Fourier Transform Spectroscopy, John Wiley & Sons, New York, 1975, pp. 311-317.

5. Mertens, F.P., "Infrared Reflectance Study of the Oxidation of Aluminum Single Crystals," Surface Sciences, 71, 161-173 (1978).

6. Wagatsume, K., Monma, K. Suetaka, W., "Infrared Emission Spectra of Thin Films on Metal Surfaces by a Polarization Modulation Method," Applications of Surface Science, 7, 281-285 (1981).

7. Chang, R.K. and Furtak, T.E., Surface-Enhanced Raman Scattering, Plenum Press, New York, 1982, 423 pp.

8. Bell, E.R., Raley, J.H., Rust, F.R., Seubold, F.H. and Vaughan, W.E., "Reactions of Free Radicals Associated with Low Temperature Oxidation of Paraffins," Discussions of the Faraday Society, 10, 242-249 (1951).

9. Chapman, I.D. and Hair, M.L., Proceedings of the Third International Congress on Catalysis, North-Holland, Amsterdam, 1965, p. 1091.

10. Oswald, A.A. and Noel, F., J. Chem. Eng. Data, 6(2), 294 (1961).

11. Hartman, G. and Seibert, F., Helv. Chim. Acta., 15, 1390 (1932).

TABLE 1

INFRARED EMISSION AND RAMAN BANDS OF DODECANE DEPOSITS FROM BOMB EXPERIMENTS

| Infrared | | | | Raman | |
|---|---|---|---|---|---|
| Aluminum Substrate | | Silver Substrate | | Silver Substrate | |
| $cm^{-1}$ | Assignment | $cm^{-1}$ | Assignment | $cm^{-1}$ | Assignment |
| 710 | $CH_2$ rock | 710 | $CH_2$ rock | | |
| 840 | Epoxy | 780 | $CH_2$ deformation | 820 | Secondary alcohol |
| 930 | Carboxyl | 850 | Epoxy | 960 | C-C stretches (alkanes) |
| 1180 | $CH_2$ wag (alkanes) | 910 | $CH_2$ wag of C=C | 1130 | C-C stretches (alkanes) |
| 1210 | $CH_2$ wag (alkanes) | 980 | $CH_2$ wag of C=C | 1250 | Epoxy |
| 1250 | $CH_2$ wag (alkanes) | 1130 | $CH_2$ wag (alkanes) | 1380 | Carboxylate salt |
| 1310 | $CH_2$ wag (alkanes) | 1180 | $CH_2$ wag (alkanes) | 1560 | Coupled C=C stretches (1540-1620) of polymers |
| 1350 | $CH_2$ wag (alkanes) | 1200 | $CH_2$ wag (alkanes) | 1600 | |
| 1380 | $CH_2$ wag (alkanes) | 1250 | $CH_2$ wag (alkanes) | 1640 | Symmetric C=C (alkyl) stretch and carboxylic acid dimer |
| 1430 | Carboxylate salt | 1290 | $CH_2$ wag (alkanes) | | |
| 1470 | $CH_3$ deformation | 1490 | $CH_3$ deformation | | |
| 1580 | Carboxyl (salt) | 1600 | Carboxyl (salt) | | |
| 1650 | Olefin C=C stretch | 1650 | Olefin C=C stretch | | |
| 1720 | Carbonyl | 1700 | Ketone or ester carbonyl | | |
| 1740 | Carbonyl | | | | |

Figure 1 NASA Lewis MJF8R Deposit Sample Holder.

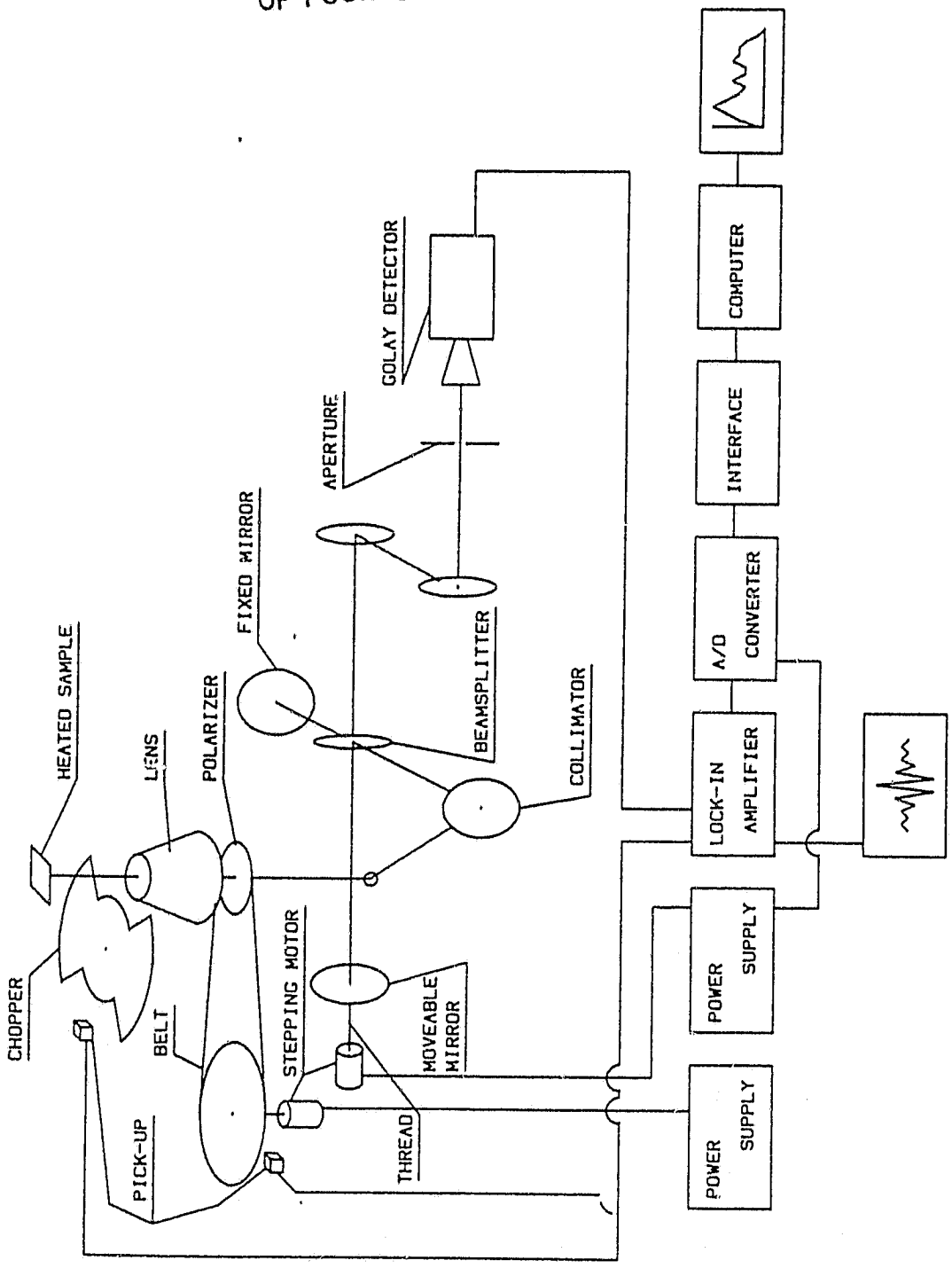


Figure 2 Schematic Drawing of Fourier Emission Microspectrophotometer

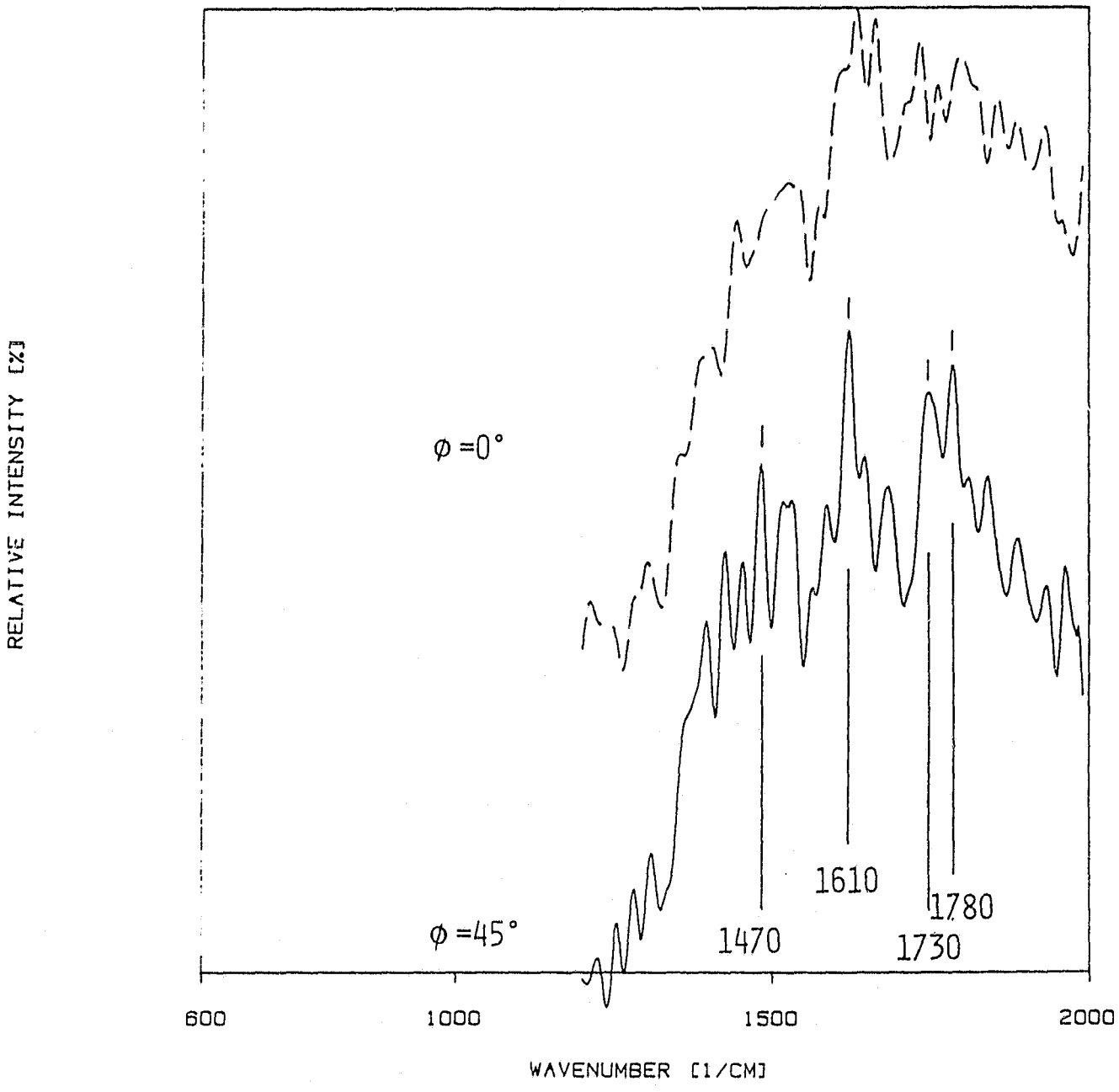


Figure 3 Change of Spectrum with Observation Angle

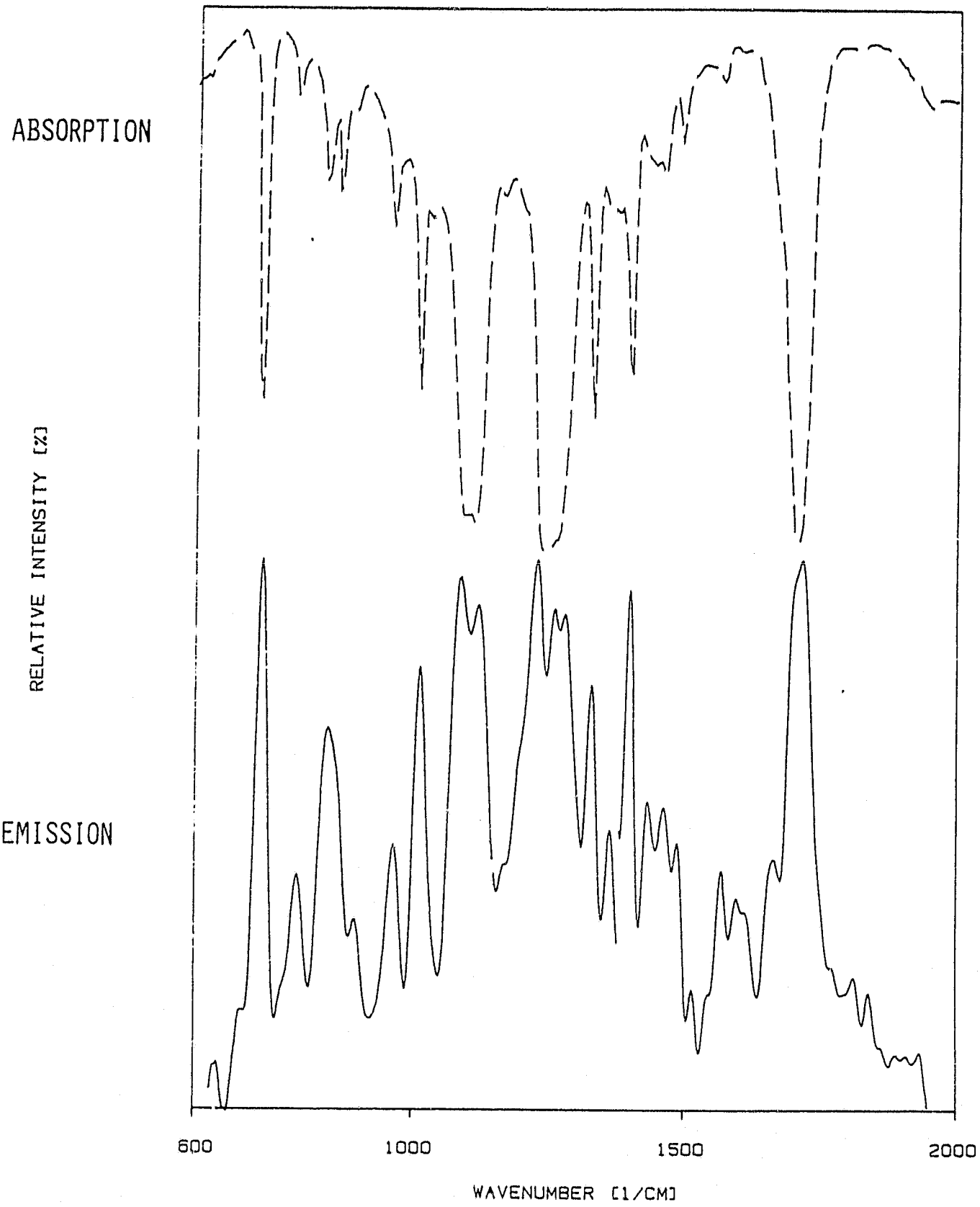


Figure 4 Absorption and Emission Spectrum of Mylar

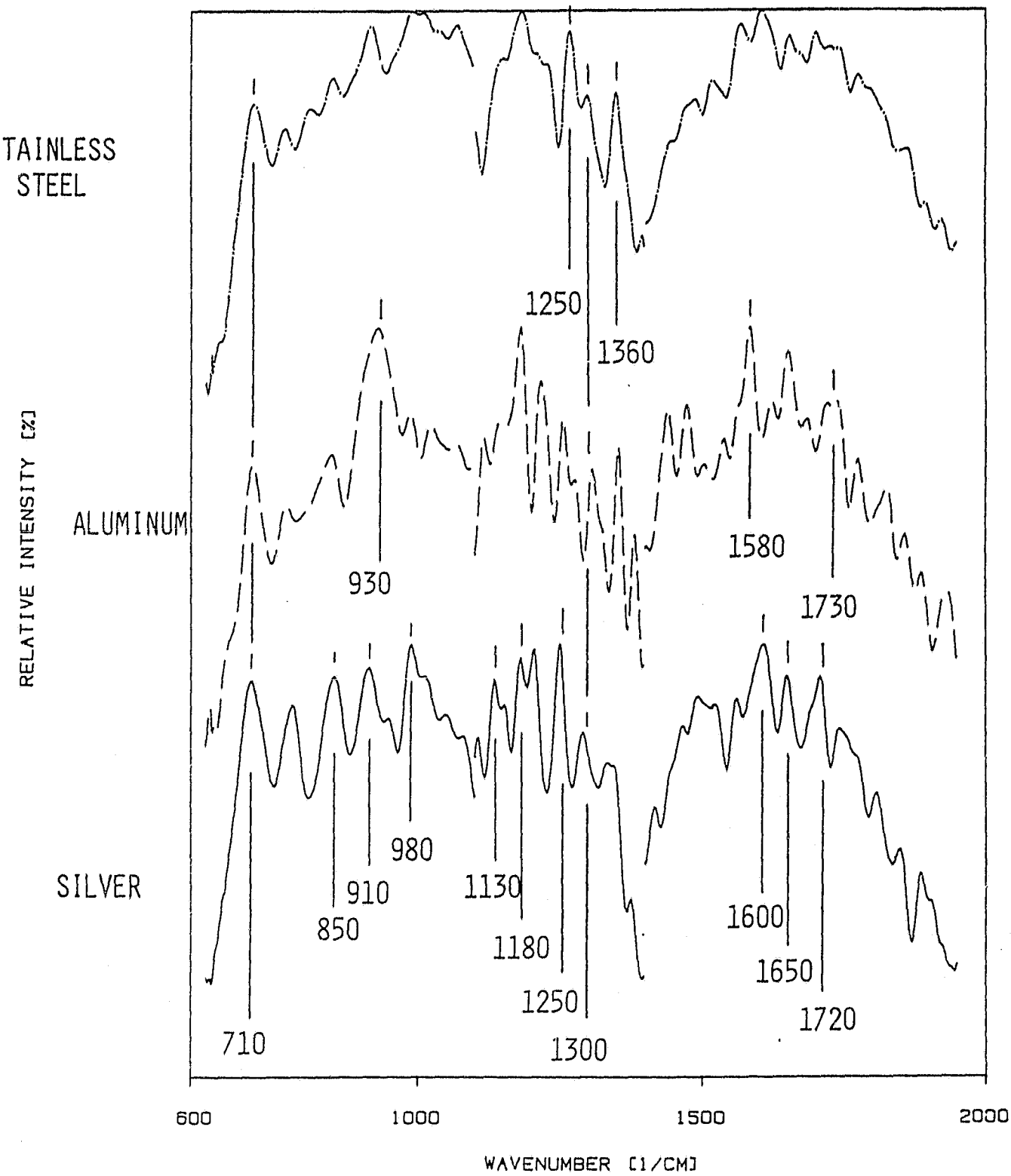


Figure 5 Emission Spectra of Dodecane Deposits Collected on Three Different Metals in a Corrosion Bomb

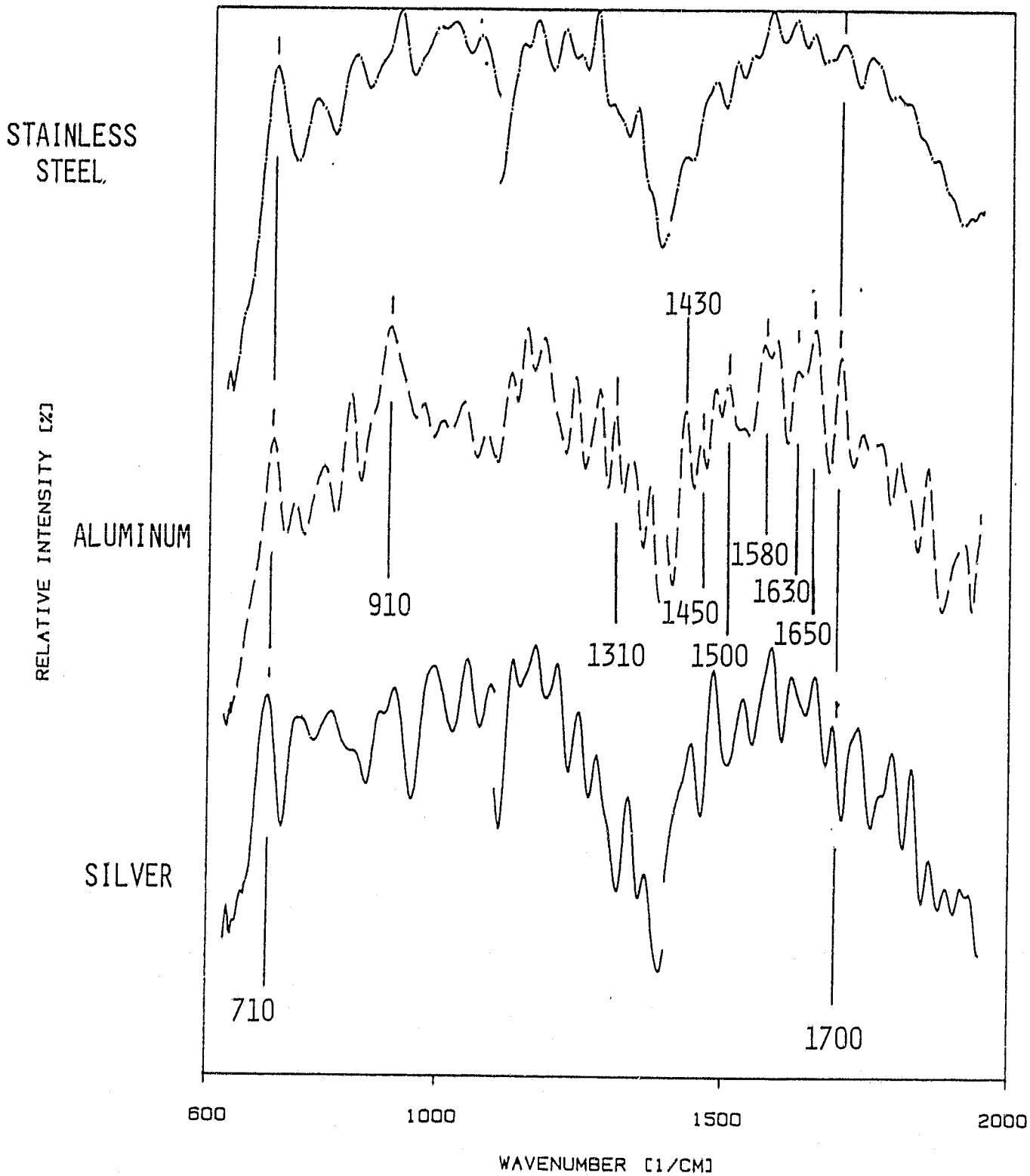


Figure 6 Emission Spectra of Toluene Deposits Collected on Three Different Metals in a Corrosion Bomb

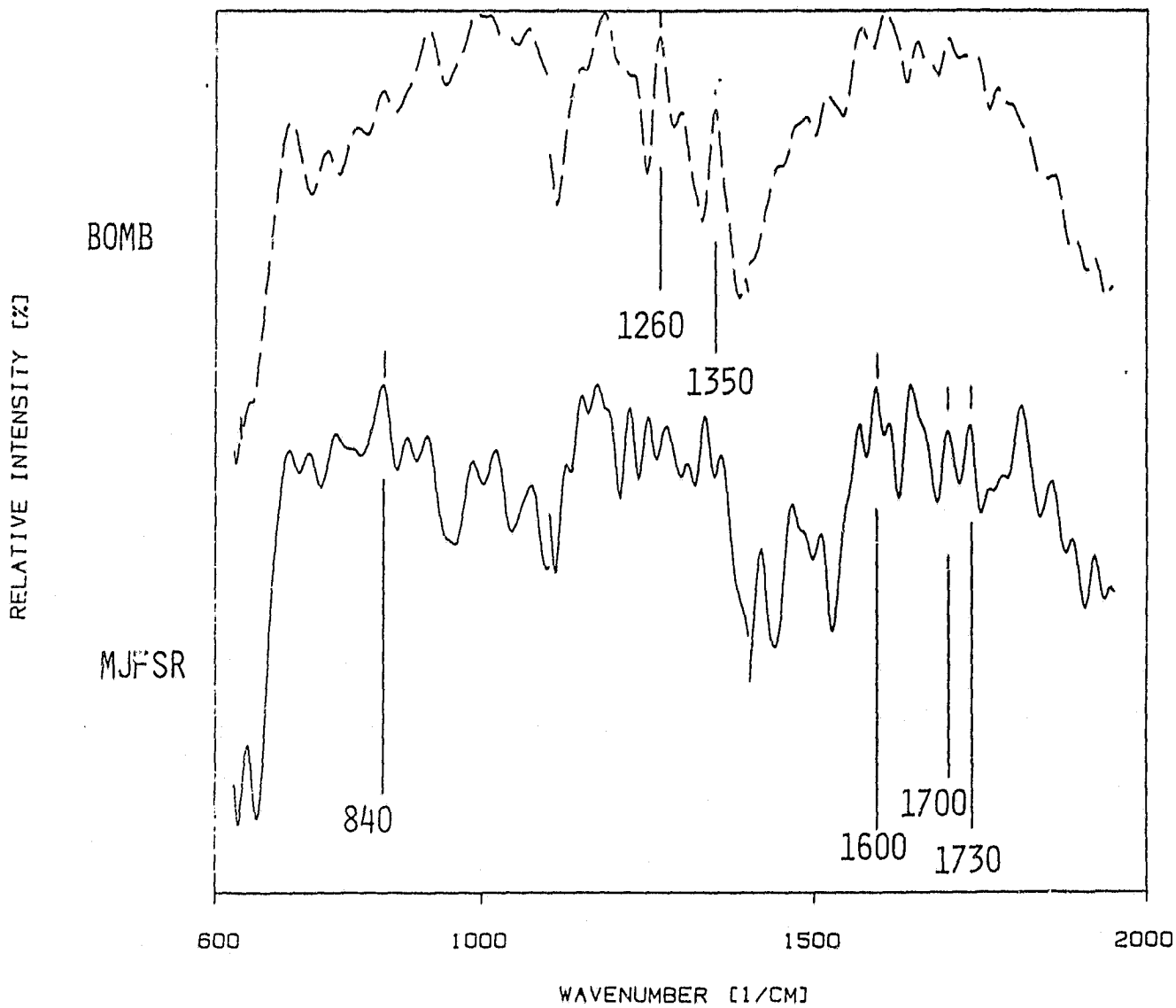


Figure 7 Comparison of Spectra from Dodecane Deposits Collected on Stainless Steel in the MJFSR and the Stainless Steel Bomb

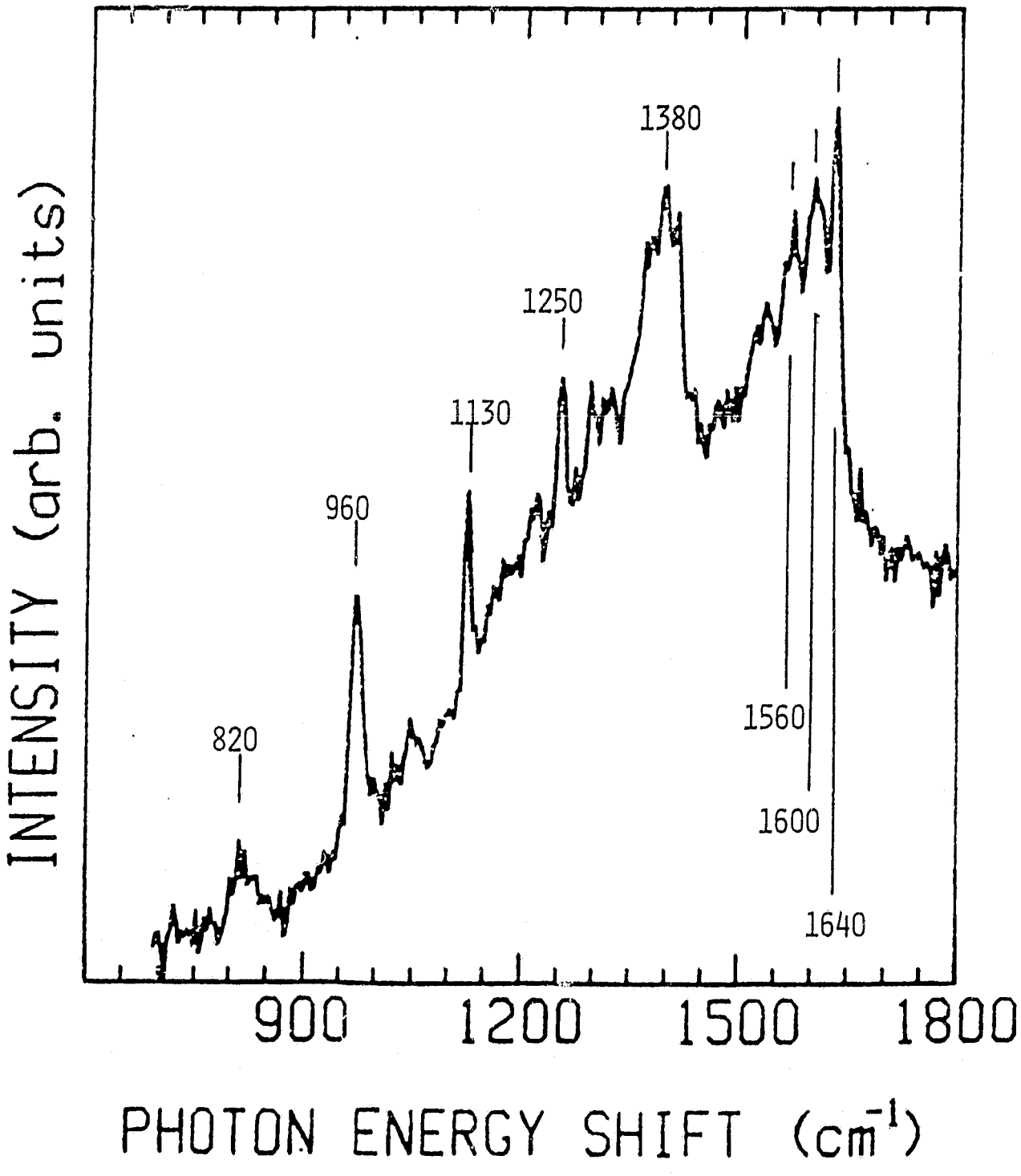


Figure 8 Raman Spectrum of a Dodecane Deposit Collected on Silver in a Stainless Steel Bomb

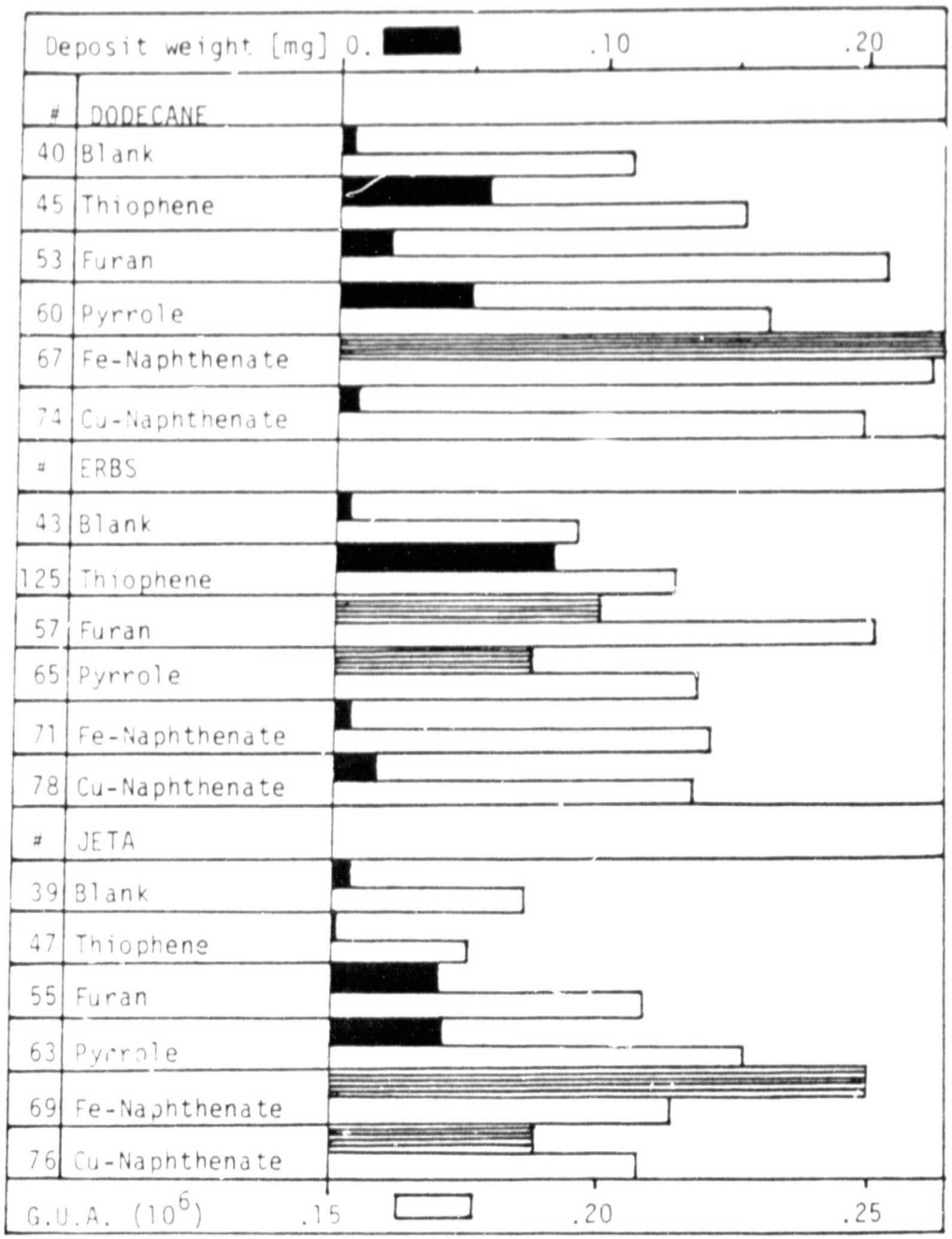


Figure 9 Comparison of MJFSR Deposit Weights and Infrared Emission Intensity (GUA). (The bars containing the horizontal lines represent weights of deposits formed on both sides of the collecting strip)

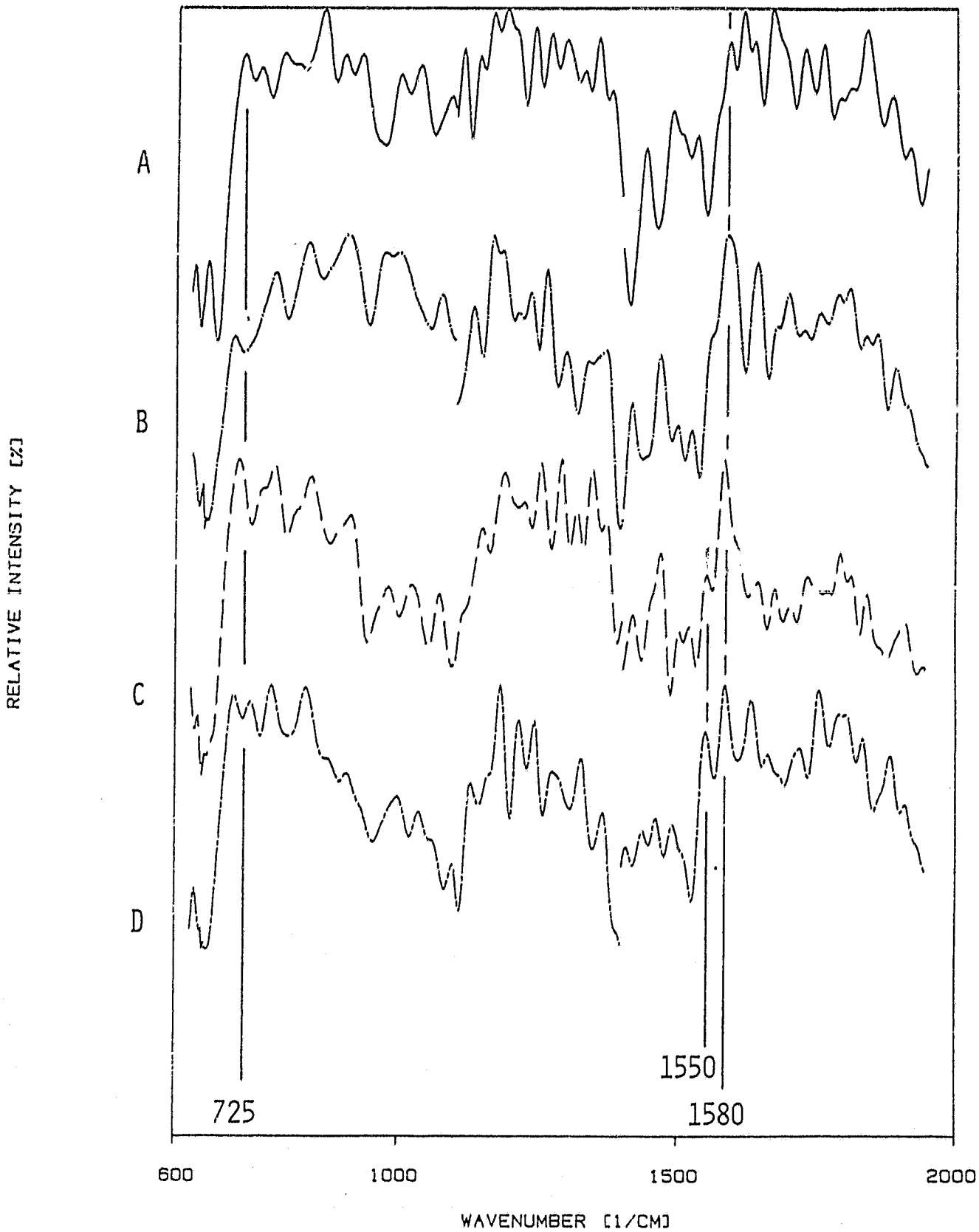


Figure 10 Emission Spectra of Dodecane Deposit on MJFSR Stainless Steel Shims (A: neat fuel, B: with copper naphthenate, C: with iron naphthenate, D: with furan)

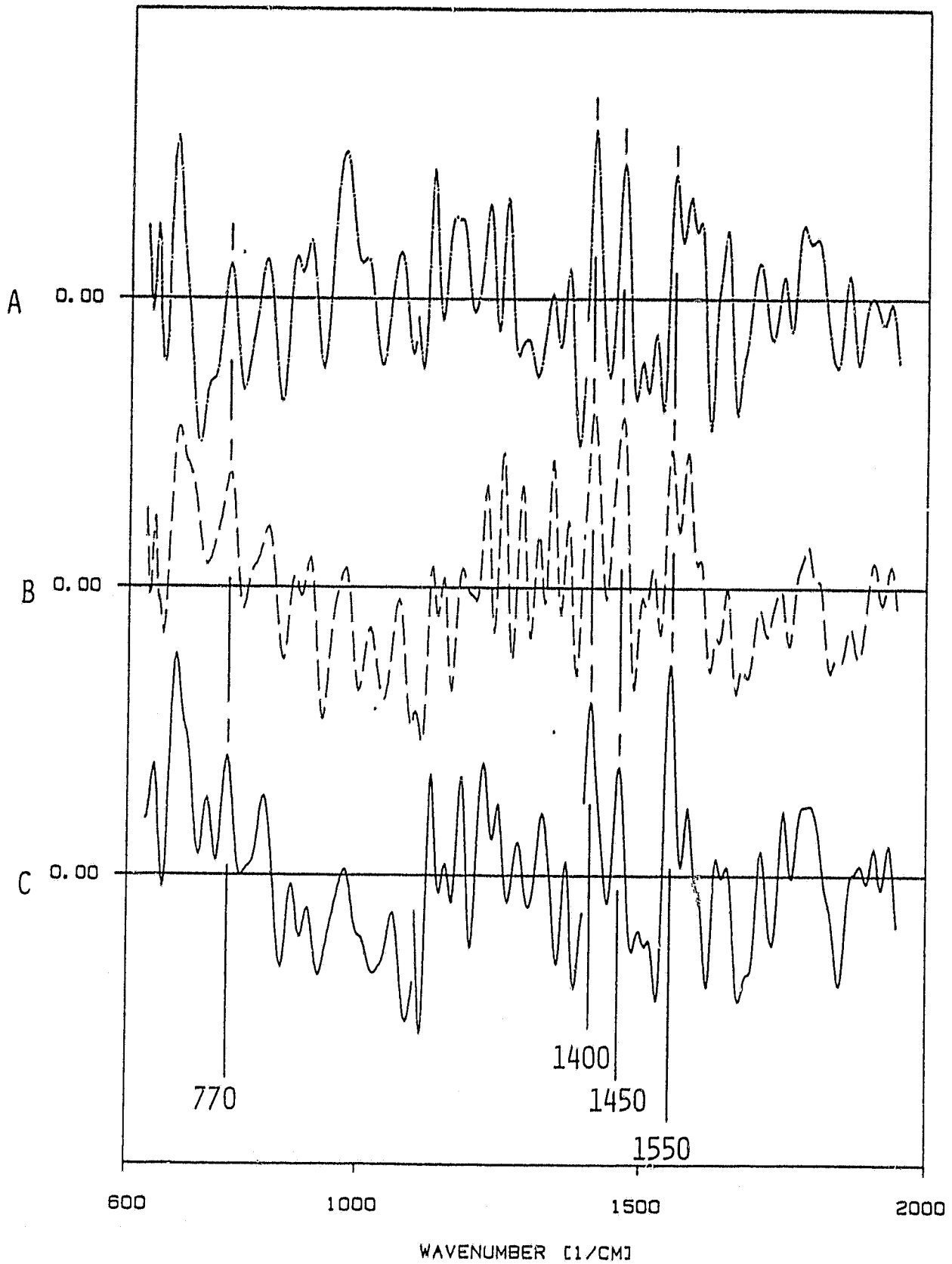


Figure 11 Difference Spectra of MJFSR Deposits from Dodecane with Additives and those of the Straight Fuel (A: with copper naphthenate minus neat, B: with iron naphthenate minus neat, C: with furan minus neat)

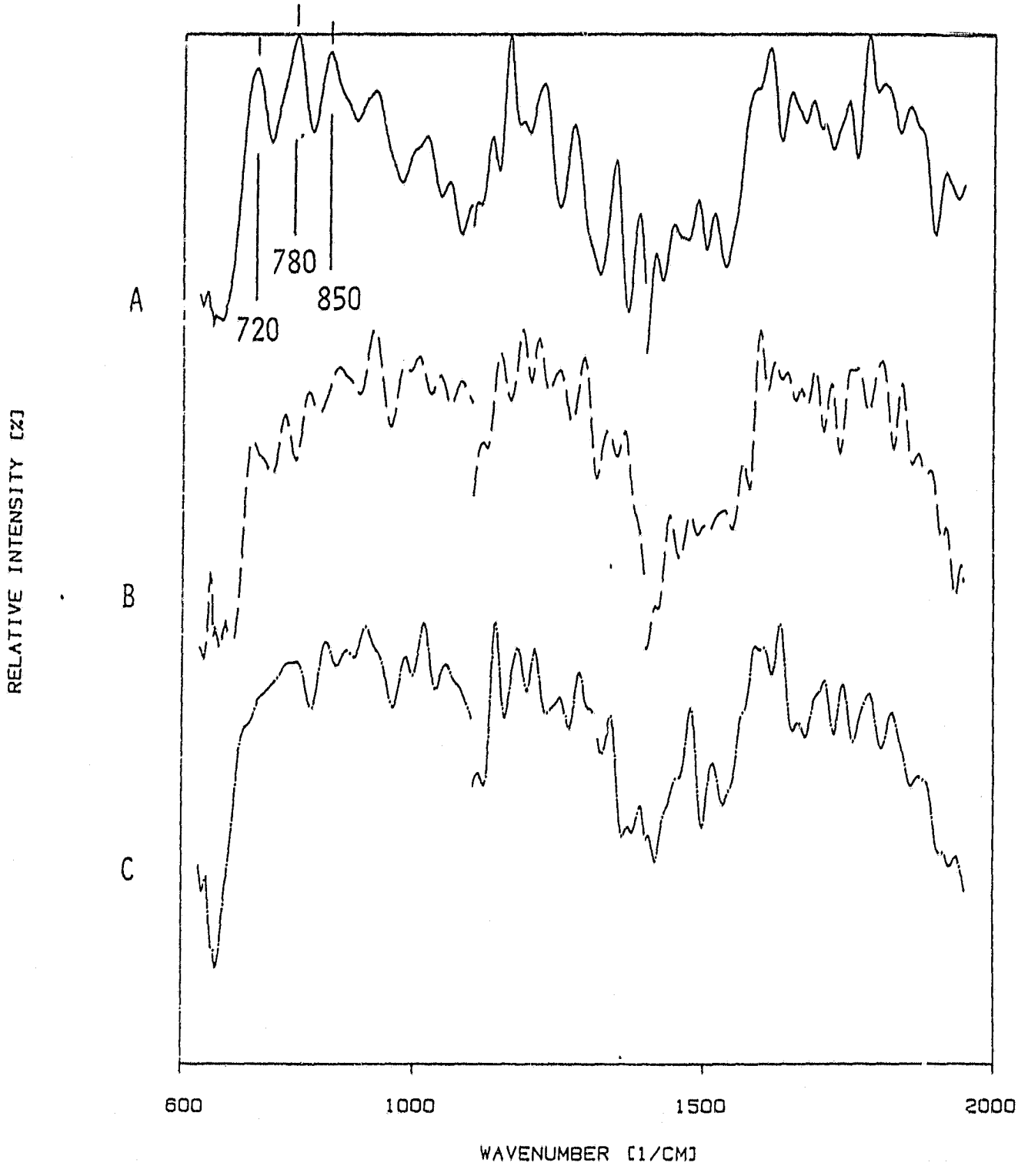


Figure 12 Emission Spectra of Jet A Fuel Deposits on MJFSR Stainless Steel Shims (A: neat fuel, B: with copper naphthenate, C: with iron naphthenate)

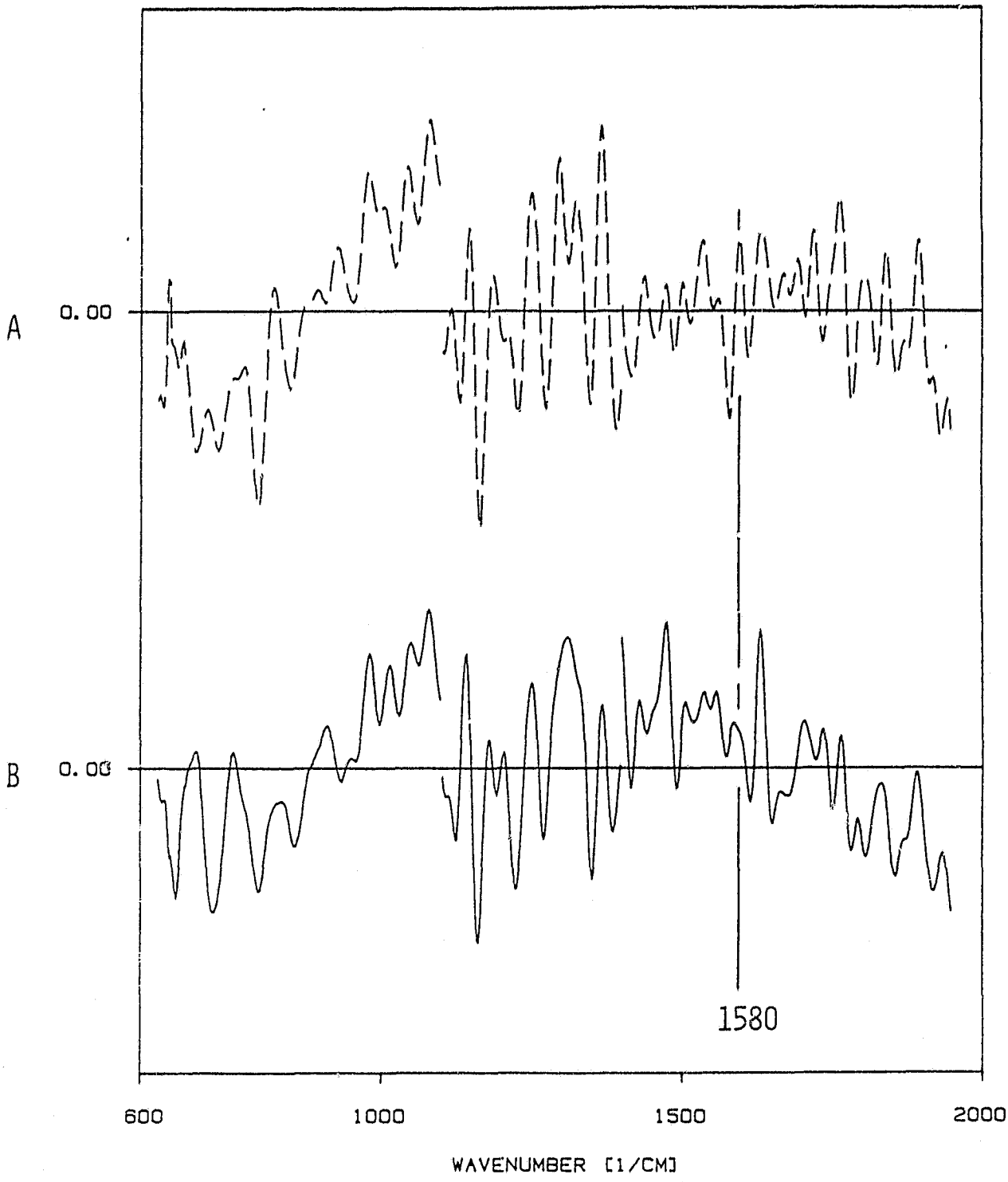


Figure 13 Difference Spectra of MJFSR Deposits from Jet A fuel with Additives and those of the Straight Fuel (A: with copper naphthenate minus neat, B: with iron naphthenate minus neat)

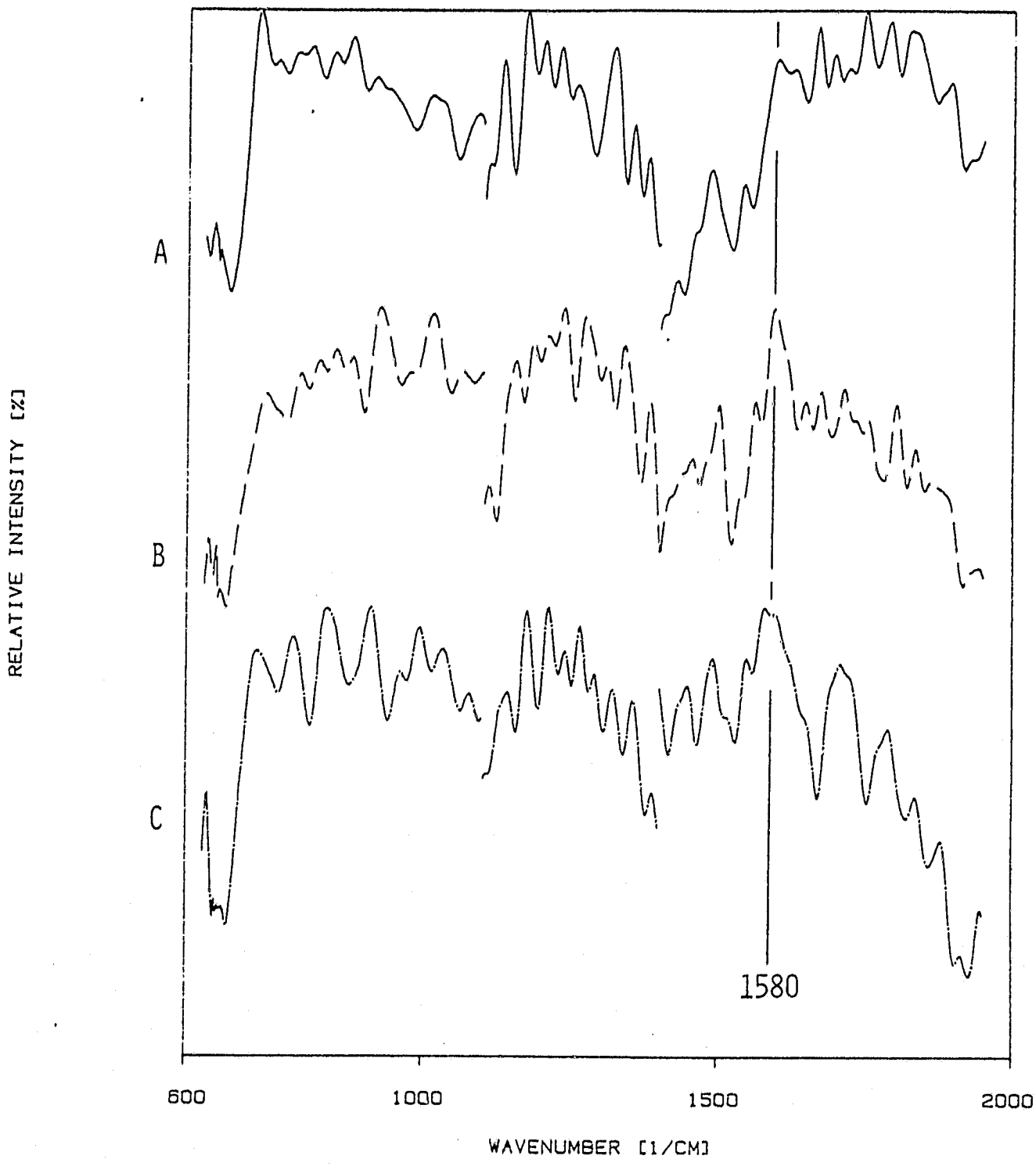


Figure 14 Emission Spectra of ERBS Fuel Deposit on MJFSR Stainless Steel Shims (A: neat, B: with copper naphthenate, C: with iron naphthenate)

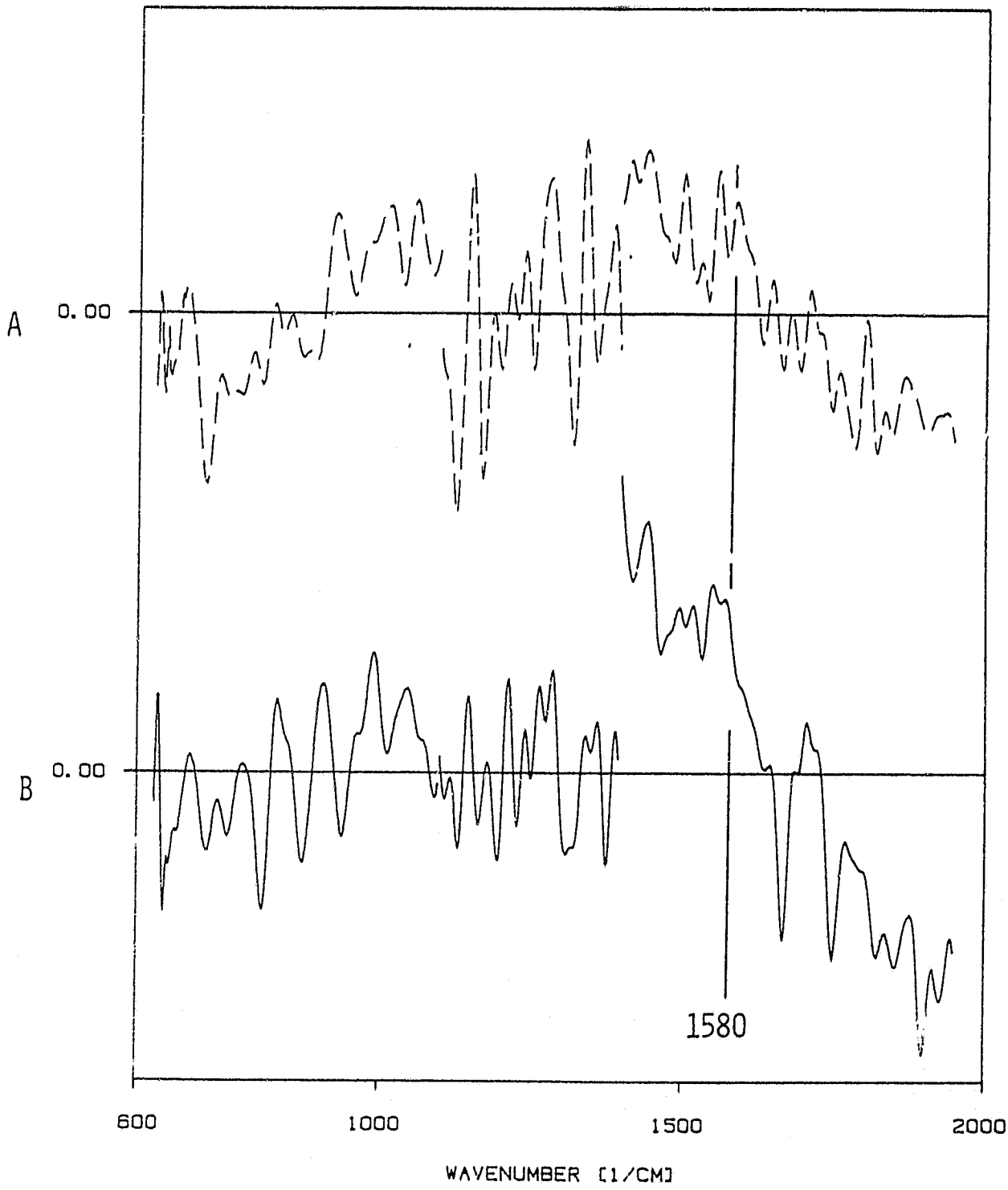


Figure 15 Difference Spectra of MJFSR Deposits from ERBS Fuel with Additives and those of the Straight Fuel (A: with copper naphthenate minus neat, B: with iron naphthenate minus neat)

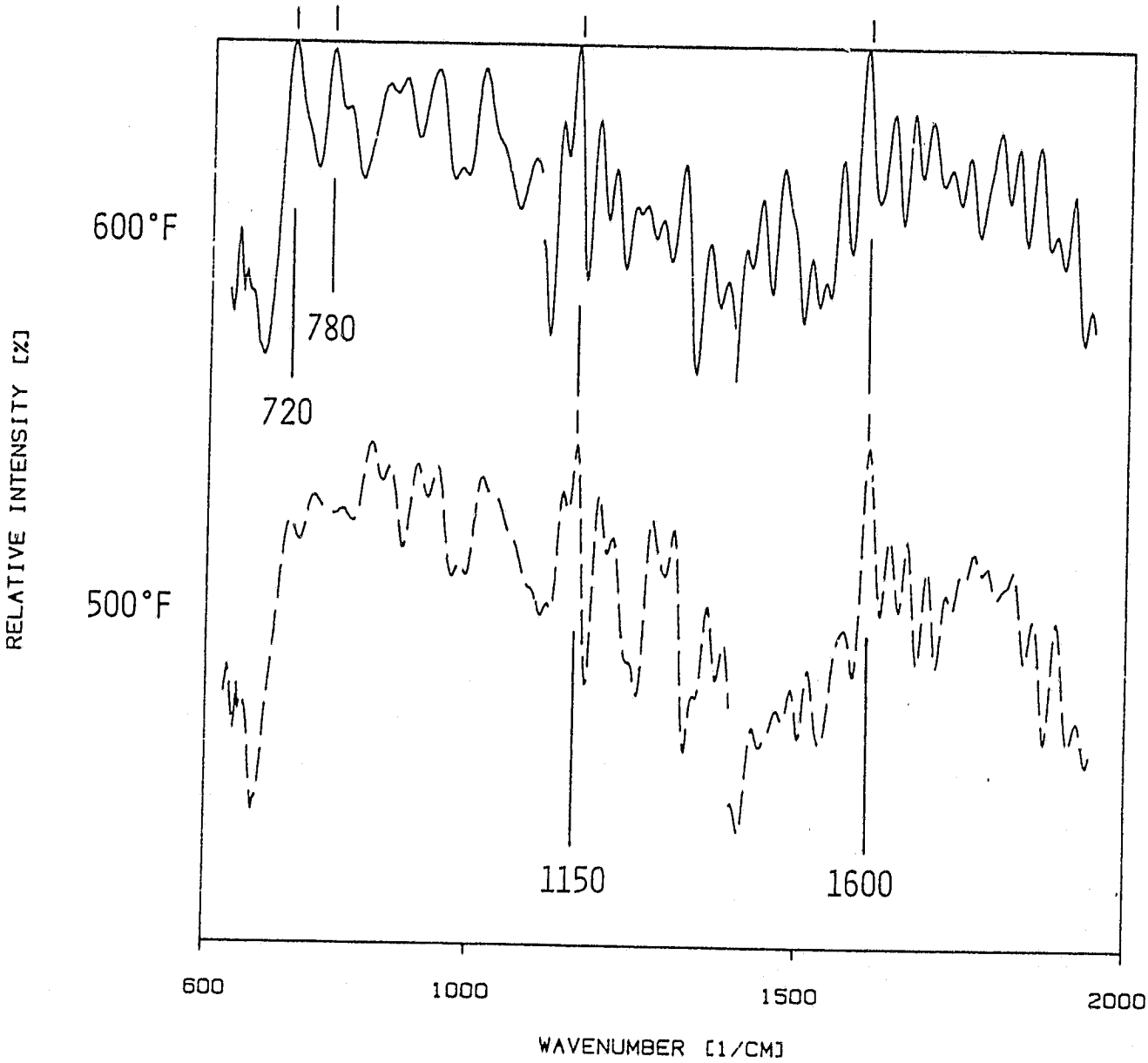


Figure 16 Emission Spectra of An ERBS Fuel Deposit Collected at 500 and 600°F